

1 **Predicting evolution using frequency-dependent selection in bacterial populations**

2 Taj Azarian^{1,2,*}, Pamela P Martinez², Brian J Arnold², Lindsay R Grant³, Jukka Corander^{4,5,6},
3 Christophe Fraser⁷, Nicholas J Croucher⁸, Laura L Hammitt³, Raymond Reid³, Mathuram
4 Santosham³, Robert C Weatherholtz³, Stephen D Bentley⁶, Katherine L O'Brien⁹, Marc
5 Lipsitch^{2,10†}, William P Hanage^{2†}

6
7 †Co-senior authors

8 9 **Affiliations:**

10 **1** Burnett School of Biomedical Sciences, University of Central Florida, Orlando, FL; **2** Center
11 for Communicable Disease Dynamics, Department of Epidemiology, T.H. Chan School of
12 Public Health, Harvard University, Boston MA; **3** Center for American Indian Health, Johns
13 Hopkins Bloomberg School of Public Health, Baltimore, Maryland; **4** Helsinki Institute for
14 Information Technology, Department of Mathematics and Statistics, University of Helsinki,
15 00014 Helsinki, Finland. **5** Department of Biostatistics, University of Oslo, 0317 Oslo, Norway;
16 **6** Infection Genomics, The Wellcome Trust Sanger Institute, Wellcome Trust Genome Campus,
17 Hinxton, Cambridge CB10 1SA, UK; **7** Big Data Institute, Nuffield Department of Medicine,
18 University of Oxford, Oxford OX3 7LF, UK; **8** MRC Centre for Global Infectious Disease
19 Analysis, Department of Infectious Disease Epidemiology, Imperial College London, London
20 W2 1PG, UK; **9** World Health Organization, Geneva Switzerland; **10** Department of
21 Immunology and Infectious Diseases, T.H. Chan School of Public Health, Harvard University,
22 Boston MA.

23
24 Pamela P Martinez pmartinez@hsph.harvard.edu

25 Brian J Arnold brianjohnarnold@gmail.com

26 Lindsay R Grant lgrant10@jhu.edu

27 Jukka Corander jukka.corander@medisin.uio.no

28 Christophe Fraser christophe.fraser@bdi.ox.ac.uk

29 Nicholas J Croucher n.croucher@imperial.ac.uk

30 Laura Hammitt lhammitt@jhu.edu

31 Raymond Reid rreid2@jhu.edu

32 Mathuram Santosham msantosham@jhu.edu

33 Robert R Weatherholtz rweather1@jhu.edu

34 Stephen D Bentley sdb@sanger.ac.uk

35 Katherine L O'Brien obrienk@who.int

36 Marc Lipsitch mlipsitc@hsph.harvard.edu

37 William P Hanage whanage@hsph.harvard.edu

38
39 **Corresponding Author:*

40 Taj Azarian, PhD MPH

41 Burnett School of Biomedical Science, College of Medicine

42 University of Central Florida

43 taj.azarian@ucf.edu

44

45 **Abstract:**

46 Predicting how pathogen populations will change over time is challenging. Such has been the
47 case with *Streptococcus pneumoniae*, an important human pathogen, and the pneumococcal
48 conjugate vaccines (PCVs), which target only a fraction of the strains in the population. Here, we
49 use the frequencies of accessory genes to predict changes in the pneumococcal population after
50 vaccination, hypothesizing that these frequencies reflect negative frequency-dependent selection
51 (NFDS) on the gene products. We find that the standardized predicted fitness of a strain
52 estimated by an NFDS-based model at the time the vaccine is introduced enables to predict
53 whether the strain increases or decreases in prevalence following vaccination. Further, we are
54 able to forecast the equilibrium post-vaccine population composition and assess the invasion
55 capacity of emerging lineages. Overall, we provide a method for predicting the impact of an
56 intervention on pneumococcal populations with potential application to other bacterial pathogens
57 in which NFDS is a driving force.

58 **Introduction:**

59 Human interventions perturb microbial populations in many ways. Most obviously, the use of
60 antibiotics or vaccines that target some strains and not others provide opportunities for new
61 strains to emerge and become established. Examples include vaccines for antigenically diverse
62 human pathogens like influenza, *Neisseria meningitidis*, *Haemophilus influenzae*, *Streptococcus*
63 *pneumoniae*, and human papillomavirus [1–3]. Predicting these changes is a central goal of
64 population genomic and evolutionary studies of pathogens [4–7]. For bacteria in particular,
65 detailed predictions of how a population will respond to a selective pressure are challenging.
66 Models that specify how mutations with a given fitness change in frequency over time are often
67 hard to apply in practice, as we typically do not know in advance important parameters such as
68 the fitness value of particular alleles or how this is affected by their frequency (frequency-
69 dependent selection) or genetic background (epistasis) [8,9].

70 Ongoing efforts to control disease caused by *Streptococcus pneumoniae* (the pneumococcus), a
71 colonizer of the human nasopharynx and a cause of pneumonia, bacteremia, meningitis, and
72 otitis media, underscore the difficulties of predicting changes after introduction of a vaccine [10].
73 Pneumococcal conjugate vaccines (PCVs) target only a fraction of this antigenically diverse
74 species, which contains over 90 distinct serotypes [11]. Following widespread introduction of

75 PCVs, non-vaccine serotypes (NVT) benefitted from the removal of their vaccine-serotype (VT)
76 competitors and became more common in carriage and disease, with the gains from reducing VT
77 disease partly offset by increases in NVT disease [12–14]. These changes in the pathogen
78 population varied by location and were not fully appreciated until retrospective analysis [15–17].

79 Our recent study of pneumococcal carriage isolates collected before and after PCV7 vaccine
80 introduction in the southwest US [17] illustrates the complexity in post-vaccine population
81 dynamics, echoing findings from other studies. Pneumococcal populations contain multiple
82 ‘sequence clusters’ which are closely related lineages, defined on the basis of sequence variation
83 in loci present among all isolates (i.e., the core genome) [18]. We henceforth use the term *strains*
84 to refer to these lineages/sequence clusters. Variation in genome content due to horizontal gene
85 transfer is a hallmark of prokaryotes; therefore, in addition to the core genome, we can define the
86 accessory genome, as those genes not found in all isolates in the sample [19,20]. Consistent with
87 their close phylogenetic relatedness in terms of core genome sequence variation, each strain we
88 identify is comprised of isolates that are fairly homogeneous – but not completely so – in the
89 presence/absence of accessory genes as well as phenotypic properties such as serotype and
90 antibiotic resistance [21].

91 Previous work showed that post-vaccine success of pneumococcal strains may depend on the
92 accessory genome [22,23]. In many bacteria, this can be a large fraction of the total number of
93 genes found in a species (i.e., the ‘pangenome’) [24,25]. A population genomic study of
94 pneumococci in Massachusetts children found that vaccination had remarkably little effect, after
95 six years, on the overall frequencies of individual accessory genes (defined as clusters of
96 orthologous genes or COGs) [23]. Despite the fact that nearly half the pre-vaccine population
97 had serotypes targeted by the vaccine, only two of >3000 loci in the accessory genome
98 significantly decreased in frequency 6 years post-introduction, and none increased [23]. More
99 recently, a geographically diverse sample of pneumococcal genomes showed that while the
100 distribution of strains varied widely across the globe, the proportion of isolates in each sample
101 containing each individual accessory gene was highly consistent across locations [22]. Where
102 vaccine was introduced, accessory gene frequencies were perturbed by the removal of vaccine
103 types but trended back toward their pre-vaccine frequencies over time [17,22,26]. Negative
104 frequency-dependent selection (NFDS) was proposed as the mechanism by which the

105 frequencies of loci were restored after vaccine introduction [22]. NFDS is a type of balancing
106 selection, which maintains diversity by favoring variants when rare, but exacting a cost when
107 they become common, such that the frequency of the variant stabilizes at intermediate values, or
108 in some instances result in frequency oscillations [9]. Examples of mechanisms produced by
109 NFDS include host immunity and bacteriophage predation, and as such, balancing selection is
110 recognized as a key contributor to population composition and diversity [27,28]. Among
111 pneumococci, similar processes have been proposed to explain the co-existence of multiple
112 serotypes [29] and vaccine-induced metabolic shifts [30].

113 Here, we present flexible, easily computable statistics that estimate the fitness of any strain using
114 the contents of its accessory genome as a proxy for how it will be affected by NFDS, dependent
115 on the frequencies of other strains in the population, and specifically of the accessory genes they
116 carry. Even though we do not know the specific loci under selection or the mechanism involved,
117 we are able to make predictions about the composition of a population as well as predict the
118 fitness of any strain in any population, whether or not it has yet appeared in that population.
119 Overall, this predictive model offers a way to study population processes and the response to
120 interventions.

121

122 **Results:**

123 In the sample of 937 pneumococcal isolates comprised of 35 strains from the southwest US, we
124 observed a sharp decline in PCV7-VT strains following vaccination (Figure 1 and S1 Figure).
125 VT strains were subsequently replaced by NVT strains, including two emergent NVT strains that
126 had not been observed pre-vaccination, although they were present during the same time period
127 in a related carriage dataset from Massachusetts [17,23]. We first show that there was
128 considerable deviation from the null expectation that NVT strains would increase in prevalence
129 *pro rata* to their pre-vaccine frequency; the most common NVT strains before vaccination were
130 not necessarily the most prevalent 12 years afterwards (Figure 1A). In particular we find 13 of 35
131 strains deviated significantly from the prevalence expected under a null *pro rata* model; 9 were
132 more common than expected and 4 less common, annotated with plus and minus signs,
133 respectively, in Figure 1B. The impact of vaccination on individual NVT strains was hence not

134 easily predictable. Consequently, public health authorities and vaccine manufacturers have had
135 to rely on post-vaccine surveillance to estimate the next epidemiologically important lineage and
136 determine subsequent vaccine formulations. At best, this uncertainty reduces the population
137 impact of vaccination; at worst, it could unintentionally increase the prevalence of virulent or
138 antibiotic resistant lineages [31].

139 Having documented that there were strains that increased significantly more or less than their
140 pre-vaccine frequency would indicate, we sought to define a parsimonious predictive algorithm
141 based on NFDS that could account for these changes. We hypothesized that evolutionary
142 dynamics could be predicted on the premise that after perturbation by vaccine, strains
143 characterized by accessory genomes that could best restore the pre-perturbation accessory-gene-
144 frequency equilibrium would have the highest fitness and therefore increase in prevalence
145 disproportionately. To this end, we implemented a deterministic model using the replicator
146 equation to calculate the fitness of a strain based on its accessory genome, using vaccination as
147 an example of perturbation [32–34] (equation 1).

$$\frac{dx_i}{dt} = x_i(\omega_i - \varphi), \varphi = \sum_{j=1}^n x_j \omega_j \quad \#(1)$$

148 Under this formulation, x_i denotes the frequency of strain i ($i = \{1, \dots, n\}$), n is the total number
149 of strains, ω_i denotes the fitness of strain i (adapted from Ref. [22]), and φ is the average
150 population fitness. The difference $(\omega - \varphi)$ is a standardized predicted fitness, and the fitness
151 vector ω is defined as the product of matrix \mathbf{K} whose element $k_{i,l}$ is a value between 0 and 1 for
152 the frequency of accessory gene l in strain i , and the vector $(e - f)$ whose l^{th} element is the
153 difference between the pre-vaccine frequency e_l and f_l , which is the gene's expected frequency
154 post-vaccination, based on removing the VTs from the pre-vaccine population, of each accessory
155 gene l (equation 2). Intuitively, the vector $(e - f)$ represents the vacancy that vaccination
156 produces in the population in terms of the accessory loci it removes, and ω_i quantifies the ability
157 of strain i to fill that gap. In contrast with previous work [22], we do not define carrying capacity
158 or migration rates, requiring only knowledge of the accessory gene frequencies at equilibrium
159 and which strains they are associated with; these quantities can be estimated from a population

160 survey prior to the perturbation of interest. We assume that the impact of recombination on the
161 accessory genome is negligible over the relatively short time period we study here.

$$\omega = \mathbf{K}(e - f) \#(2)$$

162 Using simulated data, we first assessed the ability of a strain's standardized predicted fitness
163 ($\omega - \varphi$) (for brevity we drop the modifier "standardized" hereafter) to predict the direction of its
164 change in frequency, based on its ability to resolve the vaccine-induced perturbation (Figure 2).
165 Note that this predicted fitness uses only data available before vaccine rollout. Using this model,
166 we show that in simulations, the predicted fitness is consistent with the direction of a simulated
167 strain's adjusted prevalence change (i.e. changes in prevalence minus what would be expected if
168 all NVT strains increased by the same proportion from their pre-vaccine prevalence) 92.8% of
169 cases, independent of the initial pre-vaccine frequency (Figure 2B). Next, we asked whether this
170 approach could predict the post-vaccine composition of an actual pneumococcal population, and
171 specifically the relative contribution of each strain to serotype replacement. For each strain
172 present before vaccine introduction, we used the accessory genome to calculate the fitness
173 following the removal of vaccine types. We identified 2,371 genes that were present in between
174 5% and 95% of isolates. In this data set, we found the predicted fitness value was significantly
175 and positively correlated with the observed prevalence change (Adjusted $R^2=0.41$, $p<<0.001$,
176 Figure 3A). Further, the trajectory following vaccination, whether increasing or decreasing in
177 frequency, was accurately predicted for 28 of the 31 tested strains identified in the sample, as
178 indicated by the upper right and lower left quadrants of Figure 3A. Strains with a positive
179 prevalence change had substantially higher predicted fitness than those with a negative one
180 (mean fitness of strains that increased vs. decreased 6.4 vs. -2.4; 95% CI of the difference: 5.0-
181 12.5, $p<0.001$).

182 While the predicted fitness estimates how successful each strain will be immediately following
183 vaccination, the long-term post-vaccine prevalence or change in prevalence of each strain is of
184 more direct interest for evolution and public health. Thus, we posited that over time post-
185 vaccination, gene frequencies would evolve to match as closely as possible to match those
186 present pre-vaccination, and we used an optimization technique, quadratic programming, to
187 calculate the NVT strain composition that produced accessory gene frequencies closest to those

188 observed in the pre-vaccine population. Here we specifically focused on only the 27 strains that
189 were observed pre-vaccine in the southwest US sample, allowing a projection with only data that
190 was available at the time of vaccine introduction. This approach predicted the strain composition
191 of the population following vaccination well, characterized by a 95% confidence interval of the
192 observed vs. predicted post-vaccine strain frequencies that includes the line of equality (1:1 line),
193 which denotes a perfect prediction, and by an intercept and slope that does not differ
194 significantly from zero and one, respectively ($p=0.24$; intercept 95% CI: -0.005, 0.030; slope
195 95% CI: 0.257, 1.075, Figure 3B). Similar results were obtained when comparing predicted and
196 observed change in prevalence (Figure 3C), where again the dotted line of equality fell within the
197 95% confidence interval of the regression of observed vs. predicted change in prevalence
198 ($p=0.75$; intercept 95% CI: -0.02, 0.01; slope 95% CI: 0.23, 1.36). In comparison, a naïve *pro*
199 *rata* estimate based solely on pre-vaccine prevalence performed poorly in predicting the
200 prevalence change (Figure 3D, $p=0.001$; intercept 95% CI: -0.05, -0.008; slope 95% CI: -1.43,
201 0.35). In further support of these findings we examined a previously published carriage dataset of
202 pneumococci colonizing children in Massachusetts. This dataset is imperfect in several respects.
203 First, it was smaller ($N=616$), particularly the initial sample from the population, which had only
204 131 isolates and came in the first year of vaccine introduction rather than before it; we thus refer
205 to it as “peri-vaccine.” Also making this data set less ideal, the last sample was obtained only six
206 years after the first sample, giving less time for evolution to occur than in our southwest US data
207 set. Changes in strain frequencies are shown in S2 Figure A-B. Despite the limitations of the
208 data set, applying the same quadratic programming approach we could predict the post-vaccine
209 equilibrium prevalence of the nine strains used in the analysis ($p=0.65$; intercept 95% CI: -0.05,
210 0.09; slope 95% CI: 0.25, 1.33) better than the *pro rata* model (S2 Figure C-E).

211 A further pneumococcal vaccine (PCV13) was introduced during the second half of our post-
212 vaccine sampling of the southwest US dataset [17]. Despite this, the prevalence of PCV13
213 vaccine serotypes remained largely unchanged, suggesting little impact of this vaccine over the
214 period of our study. To test the potential effect on our current analysis, we partitioned the post-
215 vaccine sample into pre- and peri-PCV13 and the results are provided in Table 1, which
216 demonstrate that our predictions were robust to sub-sampling. Finally, we tested the predictive
217 value of different genomic elements, which are linked to accessory genes, finding that core
218 genome loci ($n_{loci}=17,101$) and metabolic loci ($n_{loci}=5,853$) were also capable of predicting the

219 impact of vaccine, though not as accurately as the accessory genome based on goodness of fit
220 statistics (Table 1). This finding must be considered in the context of recombination, selection,
221 and the evolutionary timescale impacting the pneumococcal genome, which may impact the
222 varying magnitude of NFDS signal across sets of loci. Despite moderate levels of bacterial
223 recombination among pneumococci, there remains appreciable linkage disequilibrium between
224 loci nearby as well as genome-wide [8], which makes it difficult to discern the relative selective
225 importance of any particular locus. Exactly which genomic elements are responsible for the
226 predictive ability we document here is unknown but is obviously of interest and should be a
227 focus for future work.

228 **Table 1.** Comparison of pre- to post-vaccine prevalence change predictions using multiple
229 models. Goodness of fit statistics including sum of squares due to error (SSE), root mean squared
230 error (RMSE), and degrees of freedom adjusted R-squared (Adj. R²) are given for each model in
231 relation to the 1:1 line. Fit statistics are provided for the naïve *pro rata* model and quadratic
232 programming models using accessory genes, 5,853 biallelic polymorphic nucleotide sites found
233 in 272 core-genome metabolic genes, and 17,101 biallelic polymorphic nucleotide sites found in
234 1,111 core genes. The results of the sensitivity analysis using a subsample of 119 isolates
235 collected in 2010 prior to the initiation of PCV13 vaccine introduction is also presented for the
236 accessory.

| Model | n_{loci} | Adj. R ² | SSE | RMSE |
|--|------------|---------------------|-------|-------|
| <i>Pro-rata</i> (proportional change) | NA | 0.022 | 0.028 | 0.032 |
| Accessory genome (NFDS) | 2,371 | 0.223 | 0.015 | 0.024 |
| Accessory genome (NFDS) - Sensitivity analysis (2010 only) | 2,371 | 0.081 | 0.024 | 0.030 |
| Core genome (NFDS) | 17,101 | 0.173 | 0.016 | 0.024 |
| Metabolic loci (NFDS) | 5,853 | 0.154 | 0.017 | 0.025 |

237
238 In our main analysis, we can retrospectively calculate the predicted fitness of the two strains
239 (shown as SC-10 and SC-24 in Figure 1 and S1 Figure) that emerged over the study period and
240 compare them with contemporary samples collected elsewhere to determine their capacity for
241 migration and emergence. Combining the southwest US dataset with the Massachusetts dataset
242 [23,35], we identified 29 major strains and 2,511 accessory genes present between 5-95% among
243 all 1,554 taxa. The predicted fitness values in our population after vaccine introduction range

244 from -9.7 to 16.3 (median=2.5, SD=5.5) for strains present in the Massachusetts dataset. This
245 included two strains, SC-10 (serotype 19A; ST320) and SC-24 (serotypes 15A, 23A/B; ST338),
246 that were both present in the Massachusetts dataset peri-PCV7 (2001-2004) and also increased in
247 prevalence thereafter. We found that these two strains had higher predicted fitness, 8.6 and 7.2
248 respectively for SC-10 and SC-24, than any of the other potential migrant strains that were not
249 present in our southwest US sample before vaccination, indicating that their accessory gene
250 frequencies were well adapted to offset the PCV7 perturbation in the southwest US population.
251 Indeed, only two of the strains present before vaccination in the southwest US (SC-23 and SC-9)
252 had a higher predicted fitness (Figure 3). This suggests we can use this approach to quantify
253 which strains are most likely to successfully invade a population.

254 There are two primary ways in which NVT strains can fill the gap left in the population by
255 vaccination, depending on their genomic relatedness to the removed PCV7 VT strains. First,
256 NVT taxa that are closely related to VT strains in core and accessory genomes are opportune
257 replacements and are therefore expected to be more successful than average following
258 vaccination. There are two strains in our dataset that are exemplar of this, which both increased
259 after vaccination (see SC-09 and SC-23 in Figure 1 and S1 Figure). We therefore expect that for
260 any strain that contains both VT and NVT representatives, the NVT fraction will increase post
261 vaccination, especially since these NVT taxa are sometimes similar to their VT counterparts in
262 terms of serotype properties such as capsule thickness and charge, which are independently
263 correlated with prevalence [36,37]. A good example of this is the serotype 15B/C component of
264 strain SC-26 of the southwest US sample, which we now predict to be successful following the
265 more recent introduction of a vaccine incorporating six additional serotypes (PCV13) and which
266 has indeed been noted to be increasing in certain locations [38–40]. Second, where such close
267 relatives are not available, the pre-vaccine frequencies of accessory genes can be restored by
268 other NVT that are divergent in core genomes but similar in accessory genomes. This association
269 likely often results from the movement of MGEs in the population (e.g., phages and transposons)
270 or non-homologous recombination, which can make distantly related strains more similar in
271 terms of genome content. As illustrated by the pairwise comparison of core/accessory genome
272 divergence and absolute fitness difference of each strain (S3 Figure), there is an appreciable
273 range of differences in fitness for strains that are equidistant in core and accessory genome
274 divergence.

275 **Discussion:**

276 We show that by estimating the fitness of strains using an NFDS-based model and the
277 frequencies of accessory genes, we are able to predict the direction of prevalence change
278 following vaccination and more broadly the post-vaccine population composition. The ability of
279 this type of balancing selection to determine the strain composition of a population is consistent
280 with findings from environmental microbiology on multiple bacterial species [28]. Among
281 pneumococci, changes in population dynamics after the introduction of vaccine have been
282 explained by selection on many different aspects of the organism, including metabolic types,
283 antibiotic resistance, carriage duration, recombination rates, and serotype competition, all of
284 which are likely to be relevant contributors alongside, or components of, the accessory genome
285 [30,31,41,42]. We provide a simple and effective approach for estimating the fitness of any strain
286 in a population evolving under NFDS acting on accessory loci. All that is required is knowledge
287 of the strain composition of the population and the accessory loci associated with each strain, as
288 this approach does not depend on NFDS acting on particular known biological functions to
289 predict the consequences of vaccination. It is quite conceivable that a minority of loci are
290 involved, including even SNPs in the core genome, which also show a correlation (see Table 1
291 and [22]). We do not wish to imply that the sorts of selection discussed here act alone. Our
292 previous work suggests the interplay between host immunity and polymorphic protein antigens
293 may play a significant role [43], and other work suggests an important role for metabolic loci in
294 the core genome [30]. Phage predation and defense as well as antibiotic resistance all likely
295 contribute to the observed signal [21].

296 Certainly, as shown by outliers to predictions in Figure 3, we acknowledge that the model does
297 not currently capture all population dynamics. Variation among loci in the strength of NFDS
298 could account for some of these discrepancies, as indicated by retrospective model fitting. Other
299 explanations include differences in the distribution of antibiotic resistance genes or possible
300 vaccine cross-reactivity. For example, SC-18, containing serotype 6C, declined despite a positive
301 predicted fitness; however, cross-reactivity between the PCV7 6B vaccine component and 6C
302 may in part explain this observation [44]. Nevertheless, given the many potential pressures,
303 mostly not directly observable, that we might expect to structure the pneumococcal population it
304 is notable how effectively this approach can predict the impact of this perturbation. Overall, we
305 find a significant relationship between predicted fitness and the adjusted prevalence change of a

306 strain. By optimizing the prevalence of each strain conditional on the gene frequencies before
307 vaccination we can estimate the equilibrium population after vaccination, using both the
308 predicted fitness and numerical approximations of the post-vaccine equilibrium.

309 This work suggests numerous potential directions for future work, among them identifying the
310 specific accessory loci or other genomic elements that are responsible for what we observe.
311 Expanding the model to include immigration of other strains and disentangling the relative
312 contribution of selection on various loci is likely to be a fruitful area for future research. One
313 area worth exploring is the degree to which recombination acts to maintain gene frequencies on
314 the timescale of population-level shifts in lineage composition. The emergence of new strains,
315 characterized by novel combinations of accessory loci, is expected to be limited by the other
316 strains present in the population in ways that are currently not well understood.

317 Predicting evolution is a central goal of population genomics especially when related to
318 pathogens and human health. While evolutionary theory provides an understanding of bacterial
319 population processes including the relative success of lineages, distribution of phenotypes, and
320 ecological niche adaptation, these analyses are often conducted retrospectively. Here, we
321 demonstrate a method for predicting the impact of perturbing the pneumococcal population that
322 may be useful to predict the outcomes of future interventions including vaccines. By
323 incorporating information on invasive capacity, these predictions could be extended to inform
324 changes in invasive disease rates. These dynamics may suggest novel vaccine strategies in which
325 one could target those strains whose removal would result in a predicted re-equilibration that
326 favors the least virulent or most drug-susceptible lineages [45]. The pervasive finding of
327 accessory genomes in most bacterial species is usually explained by specialization of lineages to
328 specific niches; however, it could also reflect widespread NFDS, and so future work should seek
329 for evidence of similar signal in the core and accessory genome of other bacteria [46].

330 **Methods**

331 *Study population and descriptive statistics (Figure 1 and S2 Figure).*

332 The southwest US dataset used in this study is a subset of three studies of pneumococcal carriage
333 conducted among Native American communities in the southwest US from 1998 to 2012, as
334 previously described [47–49]. The pre-vaccine sample was collected from the well-defined

335 control communities of the group-randomized trial of the PCV7 vaccine [48]. Pre-vaccine
336 isolates included in our study were collected between March 1998 and April 2001. In late
337 October 2000, PCV7 vaccination became routine, including catch-up for children aged <5 years.
338 By March 2001, a total of 88% of 3–4-month old infants living in PCV7-randomized
339 communities and 77% of those in control communities had received >1 dose of PCV7 [50].
340 However, only 7 of the 274 isolates in our pre-vaccine sample were collected between October
341 2000 and March 2001; therefore, we feel it is reasonable to treat it as a pre-vaccine sample from
342 an unperturbed population. The 13-valent pneumococcal conjugate vaccine (PCV13) was later
343 introduced in 2010. The pneumococcal sample was subdivided into 35 sequence clusters (SCs),
344 referred to as strains in the main text, based on core genome diversity using hierarchical
345 Bayesian Approximation of Population Structure (hierBAPS) [51]. Secondary strain clustering
346 (e.g., A/B/C) was assigned using the second level clustering provided by hierBAPS analysis. A
347 previously described carriage dataset of pneumococcal isolates from Massachusetts, US was also
348 used to explore NFDS dynamics. For our analysis, we used the original population stratification
349 of 16 strains identified by Croucher *et al.* [23,35]. For both datasets, we then classified strains by
350 serotype composition as vaccine serotype (VT), non-vaccine serotype (NVT), or mixed (VT-
351 NVT). The methods for whole-genome sequencing and genome assembly, and population
352 genomic analysis have been described elsewhere [17].

353 For the present analysis, we focused on 937 pneumococcal carriage isolates from the southwest
354 US collected during three study periods (epochs): pre-vaccine – population equilibrium (E1,
355 1998-2001); peri-PCV7 – population perturbation (E2, 2006-2008); post-PCV7 – population
356 equilibration (E3, 2010-2012). The pre-vaccine period preceded the introduction of PCV7, while
357 peri- and post- provided snapshots 5-6 and 10-12 years, respectively, after the introduction of
358 PCV7. While the post-vaccine period includes, in part, the introduction of PCV13, we have
359 previously shown that the majority of the sample was obtained when the impact of PCV13 was
360 minimal [17]. This is supported by a sensitivity analysis to assess the effect of including all post-
361 vaccine (E3) isolates by splitting sample into pre- and post-introduction and testing
362 independently (2010 vs. 2011-2012).

363 For the additional dataset of carriage isolates from Massachusetts, we considered 133 isolates
364 collected in 2001 as E1, even though the PCV7 was introduced in these communities in 2000,

365 and 280 strains collected in 2007 as post-PCV7 (E3). Comparatively, the elapsed pre/post-
366 vaccine time (E1-E3) differed considerably, being 6 years in the Massachusetts sample compared
367 to 10-12 year in the southwest US sample. Based on previous analysis of the southwest US data,
368 accessory gene frequencies were still experiencing perturbation 5-6 years after vaccine
369 introduction (See S3 Figure in [17]). Therefore, it is likely that the Massachusetts sample had not
370 yet reached a new post-vaccine equilibrium. We considered serotypes 4, 6A, 6B, 6E, 9V, 14,
371 18C, 19F, and 23F as PCV7 vaccine-type. For each strain, we computed the proportion of PCV7
372 VT and NVT. Three serogroup 6 serotypes were included because it has previously been shown
373 that the serotype 6B component of PCV7 was cross-protective against 6A and that 6E produces a
374 6B capsular polysaccharide [52]. Further, cross-reactivity is consistent with the observed
375 elimination of 6A and 6E in the study population after the introduction of PCV7 [17].

376 The observed changes in prevalence were estimated as $x_i^3 - x_i^1$, where x_i^3 is the prevalence of
377 strain i at E3 (post-vaccine) and x_i^1 is the prevalence of strain i at E1 (pre-vaccine). As a null
378 model for vaccine impact (*pro rata* model), we calculated the expected prevalence for each strain
379 if its VT representation declined to zero in the whole population from pre- to post- vaccine, and
380 its NVT representation increased proportionately to that in the whole population, and where the
381 new NVT prevalence values g_i are renormalized to sum to one. We defined the prevalence
382 change as $x_i^3 - g_i$. To determine significant deviations of the observed post-vaccine strain
383 prevalence from the *pro rata* model, we sampled 10,000 bootstrap replicates with replacement
384 from E1, and calculated the *pro rata* prevalence changes for each replicate. We then plotted the
385 2.5%, 50%, and 97.5% quantiles of these resampled predictions in Figure 1B. We defined x_i^3 as
386 significantly different from the null expectation if the strain's prevalence change was outside the
387 central 95% of the bootstrap distribution of the predicted value.

388 *Pneumococcal pangenome analysis.*

389 As previously described, pangenome analysis of 937 taxa was carried out using Roary v3.12.0
390 [17]. The resulting presence/absence matrix was used to generate a binary accessory genome
391 alignment of 2,371 clusters of orthologous groups (COGs). This binary alignment was used to
392 infer a maximum likelihood (ML) phylogeny using RAxML v8.2 with BINGAMMA substitution
393 model and 100 bootstrap replicates [53]. The same approach was used to infer a ML phylogeny
394 of SNPs found in the core genome using the GTRGAMMA substitution model. Serotype,

395 collection period (epoch), and strain (SC) assignment were visualized in relation to the accessory
396 genome phylogeny. We then imported the phylogeny into R using APE v4.1 and computed the
397 mean pairwise patristic distance among all strains using the *meandist* function in the R package
398 Vegan v2.4-67 [54]. Hierarchical clustering of scaled between-strain patristic distances was
399 visualized using *heatmap.2* in ggplots v3.0.1. Last, core and accessory genome divergence was
400 compared to the absolute fitness difference among strains. For the additional carriage dataset
401 from Massachusetts, the presence/absence matrix was obtained from the online repository
402 available at <https://www.nature.com/articles/sdata201558>.

403 *Predicted Fitness.*

404 In the southwest US dataset, we identified 35 strains among 937 isolates. This included a
405 polyphyletic grouping of strains present at low frequencies in the overall population (SC-27).
406 Pre-vaccine, two strains (SC-10 and SC-24) were not sampled, having only been observed after
407 the introduction of vaccine. Further, two strains (SC-22 and SC-23) had no NVT component pre-
408 vaccine but did post-vaccine. For these four strains, we imputed pre-vaccine accessory gene
409 frequencies by subsampling representative taxa from the first time point when they were
410 observed (peri-vaccine period (E2) in both instances). This allowed us to calculate the fitness of
411 these strains. Three additional strains (SC-04C, SC-12, and SC-17) were excluded because they
412 had no NVT isolates present pre-vaccine or were not observed post-vaccine (i.e., they were
413 comprised solely of VT isolates); therefore, their fitness could not be imputed nor their
414 prevalence change. Finally, there were a few instances of strains that contained both VT and
415 NVT serotypes. Where this was the case, for the purposes of considering the NVT portion of
416 such strains, we removed the VTs and considered the remainder in isolation as an NVT strain.
417 This was repeated for 14 of 16 strains in the carriage dataset from Massachusetts. This required
418 imputing five strains that were not sampled pre-vaccine.

419 For the two previously unobserved strains (SC-10 and SC-24) in the primary dataset, we
420 assessed the degree to which their accessory genome composition may have contributed to
421 emergence after the introduction of PCV7 by comparing their fitness to strains found in the
422 Massachusetts dataset [23,35]. To do this, we repeated the pangenome analysis using a merged
423 dataset of 1,554 carriage isolates (including all genomes from [24]). Population structure
424 (determination of strains) of the combined sample was assessed with hierBAPS and accessory

425 gene filtering was conducted as previously detailed. Frequencies of accessory genes were
426 determined for each strain in the Massachusetts dataset, and the predicted fitness values were
427 calculated by comparing those frequencies to $(e - f)$ in the primary southwest USA dataset. The
428 distribution of fitness values in the Massachusetts dataset were assessed and compared with the
429 two emergent strains to determine their ranking. Last, to predict the impact of PCV13 on the
430 pneumococcal population, we repeated the quadratic programming analysis on the post-vaccine
431 population. To do this, we recalculated the change in strain prevalence resulting from the
432 removal of six additional PCV13 VT serotypes (1, 3, 5, 6A, 7F, 19A) and determined the
433 predicted fitness for each extant NVT strain to identify those with positive values, i.e. those that
434 will likely be more successful in the PCV13 era.

435 *Post-vaccine equilibrium frequencies via quadratic programming*

436 Using 2,371 accessory genes present in 5-95% of taxa of the southwest US dataset, we
437 determined pre-vaccine accessory gene frequencies for each strain, considering NVT taxa only.
438 For this, we focused on 27 major strains which 1) had NVT taxa present pre-vaccine and 2) were
439 not polyphyletic. This excluded eight strains (SC-04C, SC-10, SC-12, SC-17, SC-22, SC-23, SC-
440 24, and SC-27) and replicated what would have been possible with the available pre-vaccine
441 data. S4 Figure shows the distribution of the 2,371 accessory genes among isolates belonging to
442 the 27 strains. This figure was also used to test the assumption that the impact of recombination
443 on the accessory genome is negligible over our study period, where we compared the pre-vaccine
444 and post-vaccine accessory gene frequencies for each NVT strain. For the 27 strains, we
445 computed the predicted prevalence of each strain such that post-vaccine accessory gene
446 frequencies approached as closely as possible to pre-vaccine frequencies by using a quadratic
447 programming approach. Quadratic programming involves optimizing a quadratic function based
448 on several linearly constrained variables [55], and was done using the package quadprog v1.5-5
449 implemented in Rstudio v1.0.143 with R v3.3.19 [56]. Details of this implementation can be
450 found in the R code provided. This was then repeated using: 1) 17,101 biallelic polymorphic
451 sites found in 1,111 genes in the core genome and present among 5-95% of taxa and 2) 5,853
452 biallelic polymorphic sites found in 272 metabolic genes present in the core genome and present
453 among 5-95% of taxa. We then conducted a sensitivity analysis using genes present in 1-99%
454 and 2.5-97.5% of taxa and found the results did not differ significantly from those obtained using

455 genes present among 5-95% of taxa. Detailed methods for the ascertainment of genomic loci are
456 in Azarian *et al* [17].

457 Using 1,056 accessory genes present in 5-95% of taxa of the Massachusetts dataset, we
458 determined pre-vaccine accessory gene frequencies for each strain, considering NVT taxa only.
459 For this, we focused on 9 major strains, which had NVT taxa present pre-vaccine and were not
460 polyphyletic (SC-1, SC-2, SC-4, SC-8, SC-9, SC-10, SC-11, SC-12, SC-16). This excluded
461 seven strains and replicated what would have been possible with the available pre-vaccine data.
462 For the 9 strains, we computed the predicted prevalence of each strain such that post-vaccine
463 accessory gene frequencies approached as closely as possible to pre-vaccine frequencies using a
464 quadratic programming as described above.

465 For each model, we evaluated accuracy by determining if the slope and intercept of the predicted
466 and observed strain frequencies were close to one and zero, respectively. Goodness of fit
467 statistics including sum of squares due to error (SSE), root mean squared error (RMSE), and
468 degrees of freedom adjusted R-squared (Adj. R^2) were used to evaluate each model. In addition
469 to assessing how well we could predict post-PCV7 prevalence, we also tested if we accurately
470 inferred whether a strain would increase or decrease after the introduction of vaccine. To do this,
471 we calculated the observed prevalence trajectory from pre- to post-vaccine and compared that to
472 the predicted trajectory, identifying those with significantly positive or negative risk differences
473 using Fisher's exact test.

474

475 **Funding:** T.A. and W.P.H. were funded by NIH grant R01 AI106786. T.A., P.P.M. and M.L.
476 were funded by NIH grant R01 AI048935. N.J.C. was funded by a Sir Henry Dale fellowship,
477 and jointly funded by the Wellcome Trust and Royal Society (Grant Number 104169/Z/14/A).
478 J.C. was funded by European Research Council grant number 742158.

479

480 **Competing interests:** M.L. has consulted for Pfizer, Affinivax and Merck and has received
481 grant support not related to this paper from Pfizer and PATH Vaccine Solutions. W.P.H., M.L.,
482 and N.J.C. have consulted for Antigen Discovery Inc. The authors have declared that no
483 competing interests exist. K.L.OB. has received grant support for pneumococcal work not related
484 to this paper from Pfizer, GSK, and Gavi. K.L.OB. has consulted for Merck and Sanofi Pasteur.

485 L.R.G, L.L.H., and R.C.W. have received grant support not related to this paper from Pfizer,
486 Merck and GSK.

487

488 **Data and materials availability:** Whole-genome sequencing data are available from NCBI
489 under BioProject PRJEB8327: <https://www.ncbi.nlm.nih.gov/bioproject/PRJEB8327>. Accession
490 numbers and accompanying metadata have previously been published. All R code and associated
491 input data frames as well as phylogenies are available on GitHub here: [https://github.com/c2-](https://github.com/c2-d2/Projects/tree/master/NFDS)
492 [d2/Projects/tree/master/NFDS](https://github.com/c2-d2/Projects/tree/master/NFDS).

493

494 **Acknowledgements:** The ideas in this paper and the collaborative relationships underlying them
495 are owed in significant part to the Permafrost Conference on Microbial Genomics, of Blessed
496 Memory. We would also like to thank Xueting Qiu for her assistance with the manuscript
497 preparations and revisions.

498

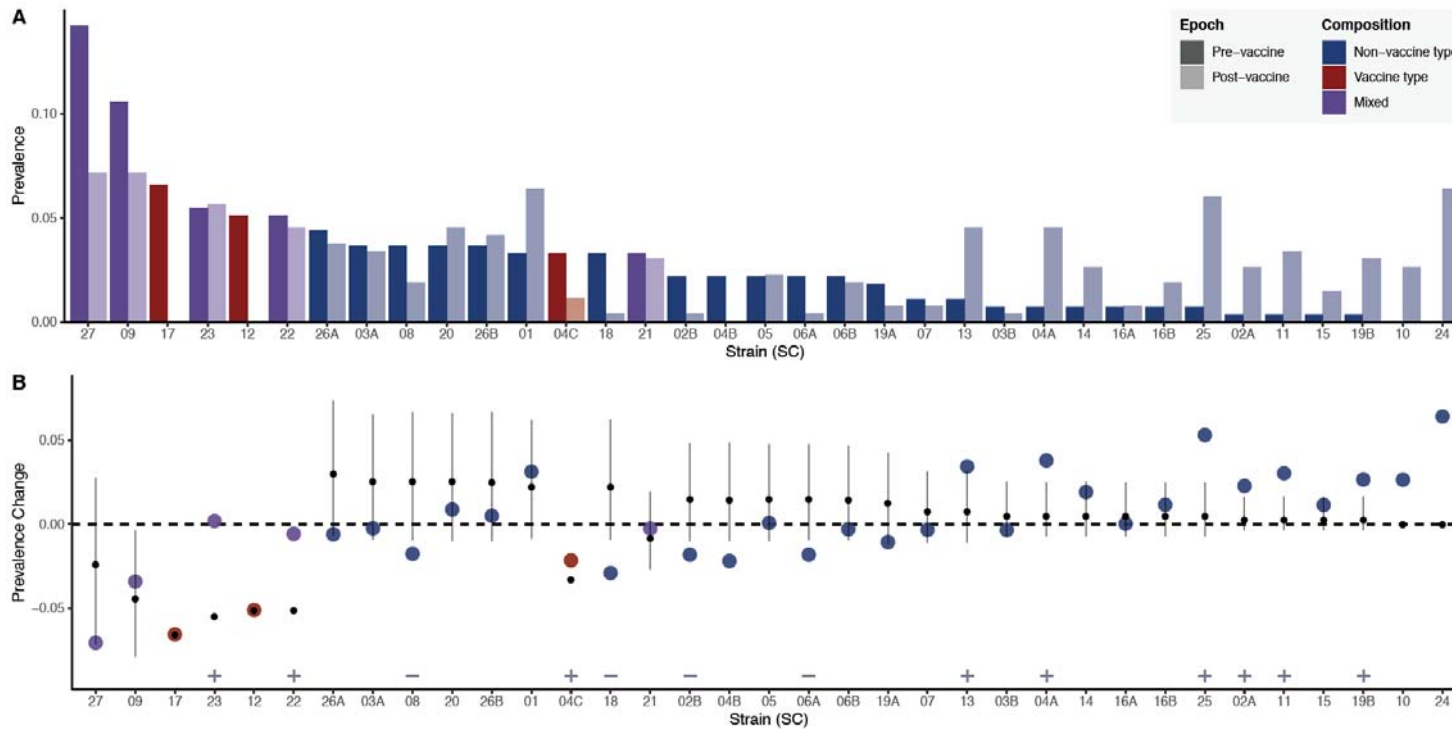
499 **References:**

- 500 1. Gray P, Palmroth J, Luostarinen T, Apter D, Dubin G, Garnett G, et al. Evaluation of HPV
501 type-replacement in unvaccinated and vaccinated adolescent females-Post-hoc analysis of
502 a community-randomized clinical trial (II). *Int J cancer*. 2018;142: 2491–2500.
503 doi:10.1002/ijc.31281
- 504 2. Menzies RI, Markey P, Boyd R, Koehler AP, McIntyre PB. No evidence of increasing
505 *Haemophilus influenzae* non-b infection in Australian Aboriginal children. *Int J*
506 *Circumpolar Health*. 2013;72: 20992. doi:10.3402/ijch.v72i0.20992
- 507 3. Hoge A, Van Effelterre T, Vyse A. Exploring the population-level impact of MenB
508 vaccination via modeling: Potential for serogroup replacement. *Hum Vaccin Immunother*.
509 2016;12: 451–66. doi:10.1080/21645515.2015.1080400
- 510 4. Levin BR, Lipsitch M, Bonhoeffer S. Population Biology, Evolution, and Infectious
511 Disease: Convergence and Synthesis. *Science* (80-). 1999;283: 806 LP – 809.
- 512 5. Morris DH, Gostic KM, Pompei S, Bedford T, Łuksza M, Neher RA, et al. Predictive
513 Modeling of Influenza Shows the Promise of Applied Evolutionary Biology. *Trends in*
514 *Microbiology*. Elsevier Ltd; 2018. pp. 102–118. doi:10.1016/j.tim.2017.09.004
- 515 6. Lässig M, Mustonen V, Walczak AM. Predicting evolution. *Nat Ecol Evol*. Nature
516 Publishing Group; 2017;1. doi:10.1038/s41559-017-0077
- 517 7. Neher RA, Bedford T, Daniels RS, Russell CA, Shraiman BI. Prediction, dynamics, and
518 visualization of antigenic phenotypes of seasonal influenza viruses. *Proc Natl Acad Sci U*
519 *S A*. National Academy of Sciences; 2016;113: E1701–E1709.
520 doi:10.1073/pnas.1525578113
- 521 8. Arnold BJ, Gutmann MU, Grad YH, Sheppard SK, Corander J, Lipsitch M, et al. Weak
522 Epistasis May Drive Adaptation in Recombining Bacteria. *Genetics*. *Genetics*; 2018;
523 genetics.300662.2017. doi:10.1534/genetics.117.300662
- 524 9. Levin BR. Frequency-dependent selection in bacterial populations. *Philos Trans R Soc*
525 *Lond B Biol Sci*. 1988;319: 459–472. doi:10.1098/rstb.1988.0059
- 526 10. Wahl B, O'Brien KL, Greenbaum A, Majumder A, Liu L, Chu Y, et al. Burden of
527 *Streptococcus pneumoniae* and *Haemophilus influenzae* type b disease in children in the
528 era of conjugate vaccines: global, regional, and national estimates for 2000-15. *Lancet*
529 *Glob Heal*. 2018;6: e744–e757. doi:10.1016/S2214-109X(18)30247-X
- 530 11. Bentley SD, Aanensen DM, Mavroidi A, Saunders D, Rabbinowitsch E, Collins M, et al.
531 Genetic analysis of the capsular biosynthetic locus from all 90 pneumococcal serotypes.
532 *PLoS Genet*. Public Library of Science; 2006;2: 0262–0269.
533 doi:10.1371/journal.pgen.0020031
- 534 12. Weinberger DM, Malley R, Lipsitch M. Serotype replacement in disease after
535 pneumococcal vaccination. *Lancet*. 2011;378: 1962–73. doi:10.1016/S0140-
536 6736(10)62225-8
- 537 13. Flasche S, Van Hoek AJ, Sheasby E, Waight P, Andrews N, Sheppard C, et al. Effect of
538 pneumococcal conjugate vaccination on serotype-specific carriage and invasive disease in
539 England: a cross-sectional study. *PLoS Med*. Public Library of Science; 2011;8:
540 e1001017.
- 541 14. Hausdorff WP, Hanage WP. Interim results of an ecological experiment—Conjugate
542 vaccination against the pneumococcus and serotype replacement. *Hum Vaccin*
543 *Immunother*. Taylor & Francis; 2016;12: 358–374.
- 544 15. Hanage WP, Bishop CJ, Huang SS, Stevenson AE, Pelton SI, Lipsitch M, et al. Carried

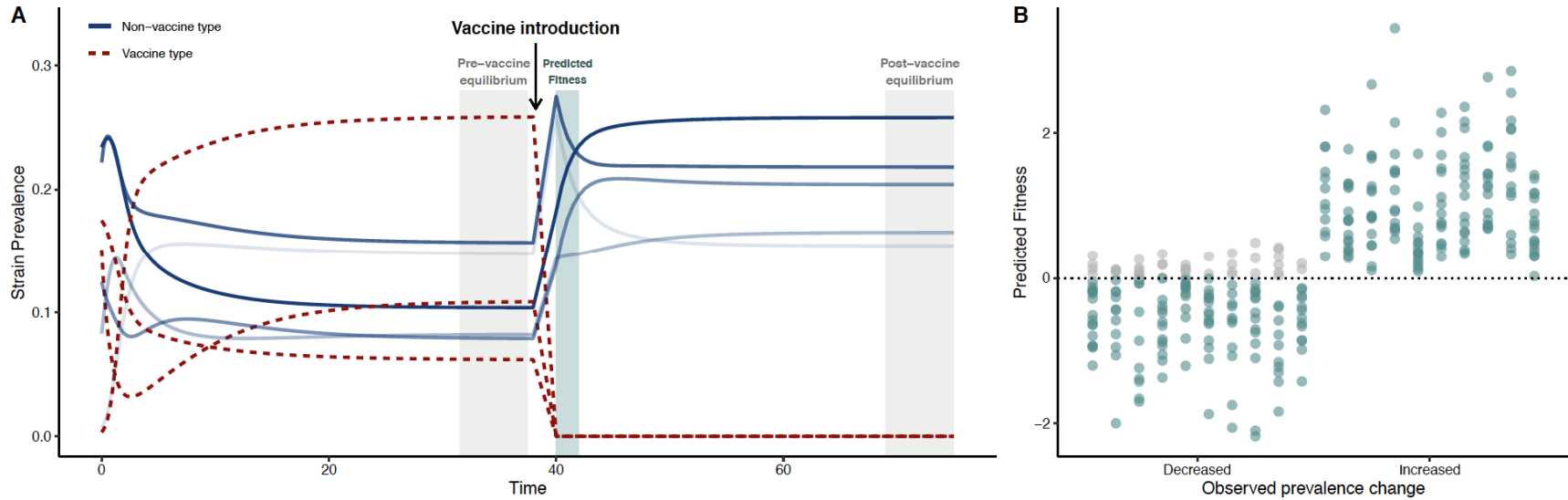
- 545 pneumococci in Massachusetts children: the contribution of clonal expansion and serotype
546 switching. *Pediatr Infect Dis J.* 2011;30: 302–8. doi:10.1097/INF.0b013e318201a154
- 547 16. Hanage WP, Finkelstein JA, Huang SS, Pelton SI, Stevenson AE, Kleinman K, et al.
548 Evidence that pneumococcal serotype replacement in Massachusetts following conjugate
549 vaccination is now complete. *Epidemics.* 2010;2: 80–84.
550 doi:10.1016/j.epidem.2010.03.005
- 551 17. Azarian T, Grant LR, Arnold BJ, Hammitt LL, Reid R, Santosham M, et al. The impact of
552 serotype-specific vaccination on phylodynamic parameters of *Streptococcus pneumoniae*
553 and the pneumococcal pan-genome. Tang C, editor. *PLoS Pathog.* Public Library of
554 Science; 2018;14: e1006966. doi:10.1371/journal.ppat.1006966
- 555 18. Cheng L, Connor TR, Siren J, Aanensen DM, Corander J. Hierarchical and Spatially
556 Explicit Clustering of DNA Sequences with BAPS Software. *Mol Biol Evol.* Oxford
557 University Press; 2013;30: 1224–1228. doi:10.1093/molbev/mst028
- 558 19. Medini D, Donati C, Tettelin H, Massignani V, Rappuoli R. The microbial pan-genome.
559 *Current Opinion in Genetics and Development.* Elsevier Current Trends; 2005. pp. 589–
560 594. doi:10.1016/j.gde.2005.09.006
- 561 20. Donati C, Hiller NL, Tettelin H, Muzzi A, Croucher NJ, Angiuoli S V, et al. Structure and
562 dynamics of the pan-genome of *Streptococcus pneumoniae* and closely related species.
563 *Genome Biol.* 2010;11: R107. doi:10.1186/gb-2010-11-10-r107
- 564 21. Croucher NJ, Coupland PG, Stevenson AE, Callendrello A, Bentley SD, Hanage WP.
565 Diversification of bacterial genome content through distinct mechanisms over different
566 timescales. *Nat Commun.* Nature Publishing Group; 2014;5: 1–12.
567 doi:10.1038/ncomms6471
- 568 22. Corander J, Fraser C, Gutmann MU, Arnold B, Hanage WP, Bentley SD, et al. Frequency-
569 dependent selection in vaccine-associated pneumococcal population dynamics. *Nat Ecol*
570 *Evol.* Nature Publishing Group; 2017;1: 1950–1960. doi:10.1038/s41559-017-0337-x
- 571 23. Croucher NJ, Finkelstein JA, Pelton SI, Mitchell PK, Lee GM, Parkhill J, et al. Population
572 genomics of post-vaccine changes in pneumococcal epidemiology. *Nat Genet;* 2013;45:
573 656–63. doi:10.1038/ng.2625
- 574 24. Tettelin H, Riley D, Cattuto C, Medini D. Comparative genomics: the bacterial pan-
575 genome. *Curr Opin Microbiol.* 2008;11: 472–7.
- 576 25. Polz MF, Alm EJ, Hanage WP. Horizontal gene transfer and the evolution of bacterial and
577 archaeal population structure. *Trends Genet.* 2013;29: 170–5.
578 doi:10.1016/j.tig.2012.12.006
- 579 26. Regev-Yochay G, Hanage WP, Trzcinski K, Rifas-Shiman SL, Lee G, Bessolo A, et al.
580 Re-emergence of the type 1 pilus among *Streptococcus pneumoniae* isolates in
581 Massachusetts, USA. *Vaccine.* NIH Public Access; 2010;28: 4842–4846.
582 doi:10.1016/j.vaccine.2010.04.042
- 583 27. Lehtinen S, Blanquart F, Croucher NJ, Turner P, Lipsitch M, Fraser C. Evolution of
584 antibiotic resistance is linked to any genetic mechanism affecting bacterial duration of
585 carriage. *Proc Natl Acad Sci.* National Academy of Sciences; 2017;114: 1075–1080.
586 doi:10.1073/pnas.1617849114
- 587 28. Cordero OX, Polz MF. Explaining microbial genomic diversity in light of evolutionary
588 ecology. *Nat Rev Microbiol;* 2014;12: 263–273. doi:10.1038/nrmicro3218
- 589 29. Cobey S, Lipsitch M. Niche and Neutral Effects of Acquired Immunity Permit
590 Coexistence of Pneumococcal Serotypes. *Science* (80-). 2012;335: 1376–1380.

- 591 doi:10.1126/science.1215947
- 592 30. Watkins ER, Penman BS, Lourenço J, Buckee CO, Maiden MCJ, Gupta S. Vaccination
593 Drives Changes in Metabolic and Virulence Profiles of *Streptococcus pneumoniae*. PLoS
594 Pathog. Public Library of Science; 2015;11: e1005034. doi:10.1371/journal.ppat.1005034
- 595 31. Obolski U, Lourenço J, Gupta S. Vaccination can drive an increase in frequencies of
596 antibiotic resistance among non-vaccine serotypes of *Streptococcus pneumoniae*.
597 Proceedings of the National Academy of Sciences of the United States of America.
598 National Academy of Sciences; 2017. pp. 1–12. doi:10.1101/135863
- 599 32. Hofbauer J, Sigmund K. Evolutionary Games and Population Dynamics. Cambridge
600 university press; 1998. doi:10.1017/CBO9781139173179
- 601 33. Taylor PD, Jonker LB. Evolutionary stable strategies and game dynamics. Math Biosci.
602 Elsevier; 1978;40: 145–156. doi:10.1016/0025-5564(78)90077-9
- 603 34. Schuster P, Sigmund K. Replicator dynamics. J Theor Biol. Academic Press; 1983;100:
604 533–538. doi:10.1016/0022-5193(83)90445-9
- 605 35. Mitchell PK, Azarian T, Croucher NJ, Callendrello A, Thompson CM, Pelton SI, et al.
606 Population genomics of pneumococcal carriage in Massachusetts children following
607 introduction of PCV-13. Microb Genomics. 2019;5. doi:10.1099/mgen.0.000252
- 608 36. Li Y, Weinberger DM, Thompson CM, Trzciński K, Lipsitch M. Surface charge of
609 *Streptococcus pneumoniae* predicts serotype distribution. Infect Immun. American Society
610 for Microbiology (ASM); 2013;81: 4519–24. doi:10.1128/IAI.00724-13
- 611 37. Hyams C, Opel S, Hanage W, Yuste J, Bax K, Henriques-Normark B, et al. Effects of
612 *Streptococcus pneumoniae* strain background on complement resistance. PLoS One.
613 Public Library of Science; 2011;6: e24581. doi:10.1371/journal.pone.0024581
- 614 38. Ho PL, Chiu SS, Law PY, Chan EL, Lai EL, Chow KH. Increase in the nasopharyngeal
615 carriage of non-vaccine serogroup 15 *Streptococcus pneumoniae* after introduction of
616 children pneumococcal conjugate vaccination in Hong Kong. Diagn Microbiol Infect Dis.
617 Elsevier; 2015;81: 145–148. doi:10.1016/j.diagmicrobio.2014.11.006
- 618 39. Richter SS, Diekema DJ, Heilmann KP, Dohrn CL, Riahi F, Doern G V. Changes in
619 pneumococcal serotypes and antimicrobial resistance after introduction of the 13-Valent
620 conjugate vaccine in the United States. Antimicrob Agents Chemother. American Society
621 for Microbiology; 2014;58: 6484–6489. doi:10.1128/AAC.03344-14
- 622 40. Kaur R, Casey JR, Pichichero ME. Emerging *Streptococcus pneumoniae* strains
623 colonizing the nasopharynx in children after 13-valent pneumococcal conjugate
624 vaccination in comparison to the 7-valent era, 2006-2015. Pediatr Infect Dis J. NIH Public
625 Access; 2016;35: 901–906. doi:10.1097/INF.0000000000001206
- 626 41. Cobey S, Lipsitch M. Pathogen Diversity and Hidden Regimes of Apparent Competition.
627 Am Nat. University of Chicago Press Chicago, IL; 2013;181: 12–24. doi:10.1086/668598
- 628 42. Lourenço J, Watkins ER, Obolski U, Peacock SJ, Morris C, Maiden MCJ, et al. Lineage
629 structure of *Streptococcus pneumoniae* may be driven by immune selection on the groEL
630 heat-shock protein. Sci Rep. Nature Publishing Group; 2017;7: 9023. doi:10.1038/s41598-
631 017-08990-z
- 632 43. Azarian T, Grant LR, Georgieva M, Hammitt LL, Reid R, Bentley SD, et al. Association
633 of pneumococcal protein antigen serology with age and antigenic profile of colonizing
634 isolates. J Infect Dis. 2017;215. doi:10.1093/infdis/jiw628
- 635 44. Grant LR, O'Brien SE, Burbidge P, Haston M, Zancolli M, Cowell L, et al. Comparative
636 Immunogenicity of 7 and 13-Valent Pneumococcal Conjugate Vaccines and the

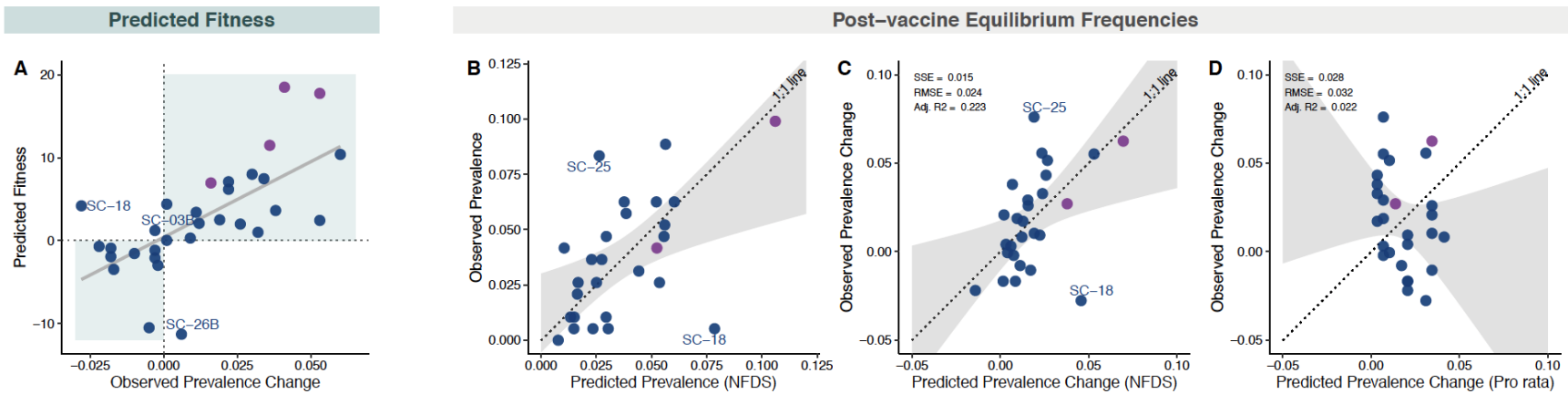
- 637 Development of Functional Antibodies to Cross-Reactive Serotypes. Borrow R, editor.
638 PLoS One. Public Library of Science; 2013;8: e74906. doi:10.1371/journal.pone.0074906
639 45. Colijn C, Corander J, Croucher NJ. Designing ecologically-optimised vaccines using
640 population genomics. bioRxiv. 2019; 672733. doi:10.1101/672733
641 46. McNally A, Kallonen T, Connor C, Abudahab K, Aanensen DM, Horner C, et al.
642 Diversification of Colonization Factors in a Multidrug-Resistant *Escherichia coli* Lineage
643 Evolving under Negative Frequency-Dependent Selection. MBio. 2019;10: e00644-19.
644 doi:10.1128/mbio.00644-19
645 47. Grant LR, Hammitt LL, O'Brien SE, Jacobs MR, Donaldson C, Weatherholtz RC, et al.
646 Impact of the 13-Valent Pneumococcal Conjugate Vaccine on Pneumococcal Carriage
647 Among American Indians. *Pediatr Infect Dis J*. 2016;35: 907–914.
648 doi:10.1097/INF.0000000000001207
649 48. O'Brien KL, Moulton LH, Reid R, Weatherholtz R, Oski J, Brown L, et al. Efficacy and
650 safety of seven-valent conjugate pneumococcal vaccine in American Indian children:
651 group randomised trial. *Lancet (London, England)*. 2003;362: 355–61.
652 doi:10.1016/S0140-6736(03)14022-6
653 49. Millar E V, O'Brien KL, Zell ER, Bronsdon MA, Reid R, Santosham M. Nasopharyngeal
654 carriage of *Streptococcus pneumoniae* in Navajo and White Mountain Apache children
655 before the introduction of pneumococcal conjugate vaccine. *Pediatr Infect Dis J*. 2009;28:
656 711–6. doi:10.1097/INF.0b013e3181a06303
657 50. Weatherholtz R, Millar E V, Moulton LH, Reid R, Rudolph K, Santosham M, et al.
658 Invasive pneumococcal disease a decade after pneumococcal conjugate vaccine use in an
659 American Indian population at high risk for disease. *Clin Infect Dis*. 2010;50: 1238–46.
660 doi:10.1086/651680
661 51. Cheng L, Connor TR, Sirén J, Aanensen DM, Corander J. Hierarchical and spatially
662 explicit clustering of DNA sequences with BAPS software. *Mol Biol Evol*. 2013;30:
663 1224–1228. doi:10.1093/molbev/mst028
664 52. Burton RL, Geno KA, Saad JS, Nahm MH. Pneumococcus with the “6E” cps Locus
665 Produces Serotype 6B Capsular Polysaccharide. *J Clin Microbiol*. 2016;54: 967–71.
666 doi:10.1128/JCM.03194-15
667 53. Stamatakis A. RAxML version 8: A tool for phylogenetic analysis and post-analysis of
668 large phylogenies. *Bioinformatics*. 2014;30. doi:10.1093/bioinformatics/btu033
669 54. Paradis E, Claude J, Strimmer K. APE: Analyses of Phylogenetics and Evolution in R
670 language. *Bioinformatics*. Oxford University Press; 2004;20: 289–290.
671 doi:10.1093/bioinformatics/btg412
672 55. Frank M, Wolfe P. An algorithm for quadratic programming. *Nav Res Logist. Wiley*
673 *Online Library*; 1956;3: 95–110.
674 56. Nocedal J, Wright SJ. *Sequential quadratic programming*. Springer; 2006.
675



676
 677
 678
 679
 680
 681
 682
 683
 684
 685
 686
 687
 688
 689
 690
 691



692
 693 **Figure 2. A.) Conceptual diagram for simulations.** Descriptive representation of the strain prevalence at different stages relative to vaccine
 694 introduction: pre-vaccine equilibrium, vaccine introduction, and post-vaccine equilibrium. We modeled a population of VT and NVT strains
 695 (represented as unique genotypes with alleles 1 or 0 at a locus, denoting the presence or absence of a single accessory locus) and simulated the
 696 removal of VT genotypes, following the post-vaccine population to equilibrium (details in methods). In this illustrative figure, eight strains
 697 are shown, with their prevalence in the population evolving over time. The system is allowed to evolve until it reaches a steady state ('pre-vaccine
 698 equilibrium'). Three strains were then targeted to mimic a vaccine introduction, which removes them from the system. The predicted fitness
 699 was then estimated from the period just after the vaccine introduction, when the population has been depleted of VT but relative prevalence of NVT
 700 has not changed – a quantity that can be calculated from pre-vaccine data alone. Finally, the system reaches a second steady state ('post-vaccine
 701 equilibrium'). Different shades of blue represent the rank of the strain frequencies in the post-vaccine equilibrium. **B.) Simulation results.**
 702 Comparison of the direction of prevalence change of strains from pre- to post-vaccine using simulated data and predicted fitness from these
 703 simulated data. For these 10 replicate simulations, 2,371 accessory loci and 35 randomly chosen strains were simulated, including three VT
 704 genotypes. For each replicate, the pre-vaccine equilibrium frequencies of the 2,371 accessory loci were varied. Final prevalence of strains were
 705 obtained by quadratic programming, and prevalence change for each NVT strain was calculated as post-vaccine prevalence minus pre-vaccine
 706 prevalence, in both cases with all NVT strains summing to 100%. Each column in the decreased and increased category represents the results from
 707 one simulation (i.e., the first column in the decreased category corresponds to the first column in the increased category and the dots sum to
 708 32). The predicted fitness of the strain accurately predicts the direction of the prevalence change in 92.8% of cases (teal dots). Grey dots represent
 709 instances where the direction of the prevalence change was not predicted correctly in the simulation.
 710



711
712

713 **Figure 3. A.) Relationship between predicted fitness and observed prevalence change from pre- to post-vaccine among 31 strains, in each**
 714 **case summing to 100%.** Prevalence change was calculated as post-vaccine frequencies minus pre-vaccine frequencies. Predicted fitness was
 715 calculated using data solely from the pre-vaccine sample, with the exceptions of strains for which there were no non-vaccine serotype (NVT)
 716 isolates present in the sample before the introduction of PCV7 (n=4). For those strains, data were imputed from the time point during which they
 717 were first observed. Four strains were excluded either because they were polyphyletic (SC-27) or had no NVT isolates present pre- or post-
 718 vaccine, and therefore could not be imputed (SC-04C, SC-12, and SC-17). The points are colored by serotype composition of strains: NVT only
 719 (blue) and mixed vaccine serotype (VT) and NVT (purple). The shaded quadrants indicate regions of accurate prediction of the prevalence change
 720 direction (increased post-vaccine vs. decreased) given the predicted fitness value. Three outlier strains are annotated for which the predicted
 721 direction of their prevalence change differed from that which was observed (i.e., they were predicted to increased based on their fitness when their
 722 prevalence from pre- to post-vaccine decreased, or vice-versa). **B.) Scatterplot of observed versus predicted prevalence of 27 strains at post-**
 723 **vaccine equilibrium based on quadratic programming.** These 27 strains contained at least one NVT strain pre-vaccine. Points are colored based
 724 on serotype composition as described in panel A. Perfect predictions would lie on dotted line of equality (1:1 line). The shaded grey region shows
 725 the confidence interval from the linear regression model used to test for deviation of the observed vs. predicted values compared to the 1:1 line.
 726 Two outliers are annotated for which the difference between their predicted and observed prevalence was >1.5 times the interquartile range of the
 727 distribution of predicted and observed prevalence differences. As a note, the predictions remained significant if SC-09 (the extreme strain at 10%
 728 prevalence in B) was removed (slope, 95% CI: 0.021, 1.05; intercept, 95% CI: -0.003, 0.03; p=0.19, chi-squared=3.5). **C-D.) Comparison of the**
 729 **predicted prevalence change from quadratic programming analysis using accessory genes and naïve *pro rata* model as shown in Figure**
 730 **1B, but applied to just these 27 strains.** The dotted line of equality (1:1 line) and confidence interval (grey) are shown as in panel B. Goodness
 731 of fit statistics including sum of squared errors (SSE), root mean squared error (RMSE), and degrees of freedom adjusted R-squared (Adj. R²) are
 732 given for each model. The lower SSE and RMSE indicate a better model fit.